Chemical Relaxation Spectrum of Glutamic Aspartic Aminotransferase/*erythro*-β-Hydroxyaspartate*

Georg H. Czerlinski and Jutta Malkewitz

ABSTRACT: The reaction of pig heart glutamic aspartic aminotransferase with the inhibitor DL-*erythro*-β-hydroxyaspartic acid was investigated employing a revised temperature-jump apparatus with detection of absorption changes at 505 mμ. Three relaxation processes demonstrated the presence of at least three enzyme-inhibitor complexes according to $E + A \underset{k_2}{\overset{k_1}{\rightleftharpoons}} EA \underset{k_4}{\overset{k_3}{\rightleftharpoons}} X \underset{k_6}{\overset{k_5}{\rightleftharpoons}} Y (\rightleftharpoons E' + A')$. Velocity constants, equilibrium constants, and enthalpies of the individual steps are summarized in Table I. Discussion of the data and a proposed reaction scheme lead to an increased probability of the presence of more reaction steps than derived thus far. These reaction steps are also expected to be present in a system with natural substrates.

The reaction of glutamic aspartic aminotransferase with some β-substituted aspartic acid analogs was investigated by Jenkins (1961). He demonstrated that the DL-*erythro* isomer of β-hydroxyaspartic acid was reacting with the pyridoxal form of the glutamic aspartic aminotransferase to yield the products and a compound absorbing in a wavelength region which is above the formerly known absorption region for this enzyme system. He obtained $\lambda_{max} = 492$ mμ and inferred that the colored complex is generally an intermediate in the reaction.

In order to investigate this intermediate in more detail, we decided to apply the temperature-jump method to this system. Our hope was also to eventually obtain more information on the details of the operation of the enzyme. The existence of a complex with an absorption peak near 490 mμ in a *natural* aminotransferase system was demonstrated first on the glutamic alanine aminotransferase system by Jenkins (1963).

These recent findings made the investigations on the above-mentioned system even more interesting. Hammes and Fasella (1962, 1963) investigated the natural system formerly employing the temperature-jump method, but they had difficulties in the evaluation because of the overlap of absorption spectra of different species and the strong interference from neighboring relaxation processes.

Methods

Instrumental. The temperature-jump apparatus used was similar to the one which was formerly described (Czerlinski, 1962). This compact, coaxial apparatus was developed from the original design of Czerlinski and Eigen (1959). Observations were performed by following the changes in transmission at 505 mμ employing a double-band interference filter of Schott and Gen., Mainz, Germany. A tungsten lamp was used. The principal difference from former data retrieval is the employment of a switching circuit, which "grounds" out the signal up to the moment when the actual relaxation process under observation starts to appear. This also permits the use of only one detection channel. The details and the signal-to-noise properties of such a circuit are discussed in another paper (Czerlinski and Nadler, 1965).

Chemicals. Pig heart glutamic aspartic aminotransferase (electrophoretically pure) was generously supplied by Dr. W. T. Jenkins, University of California, Berkeley. We determined the concentrations of the active sites of the enzyme samples by various methods. Initially, we used the method of Velick and Vavra (1962). Later, we also used the method of Jenkins (1964), employing as the molar extinction coefficient for the active sites the value 8200 M^{-1} cm^{-1} at 360 mμ. For comparison we also measured the extinction at 280 mμ and employed the ratio of the extinction at the two wavelengths for comparing the purity of enzyme samples.

After we had discovered some differences among the various methods we decided to develop our own method for titrating the concentration of active sites. The method is demonstrated by the sample curve, shown in Figure 1. We found that the results from our titrimetric determinations were in good agreement with those obtained from absorption measurements at 360 mμ. For all the measurements reported here we used this titrimetric method and assumed that only the L isomer of the racemic mixture of *erythro*-β-hydroxyaspartic acid reacts with the active site of the enzyme to give the 492-mμ band.

erythro-β-Hydroxyaspartic acid was generously

* From The Johnson Research Foundation for Medical Physics, University of Pennsylvania, Philadelphia. *Received December 18, 1964.* The investigations were supported by a grant from the U.S. Public Health Service (GM10888). Preliminary reports on this project have been published previously (Czerlinski, 1964a; Czerlinski *et al.*, 1964).

supplied by Dr. W. T. Jenkins, and we established our concentrations gravimetrically, assuming that 149 represents the proper molecular weight of this inhibitory substrate. Sodium tetraborate (0.02 M in the final mixture + K_2SO_4 [Baker Analyzed Reagent] → μ = 0.1) was reagent grade and obtained from Merck and Co., Inc. The *p*H was adjusted with H_2SO_4 from Baker Chemical Co. We redistilled ordinary distilled water according to a method described earlier (Czerlinski and Schreck, 1964). For the temperature-jump experiment, a thermostat was used which kept the temperature at 20°. The enzyme was added to each individual mixture at the end immediately before the filling of the cell. The signal S_T was determined and only a few temperature jumps were done per mixture. The whole procedure took only a few minutes, not enough time for any appreciable degeneration of the keto form of the inhibitory substrate (S_T generally constant within experimental time).

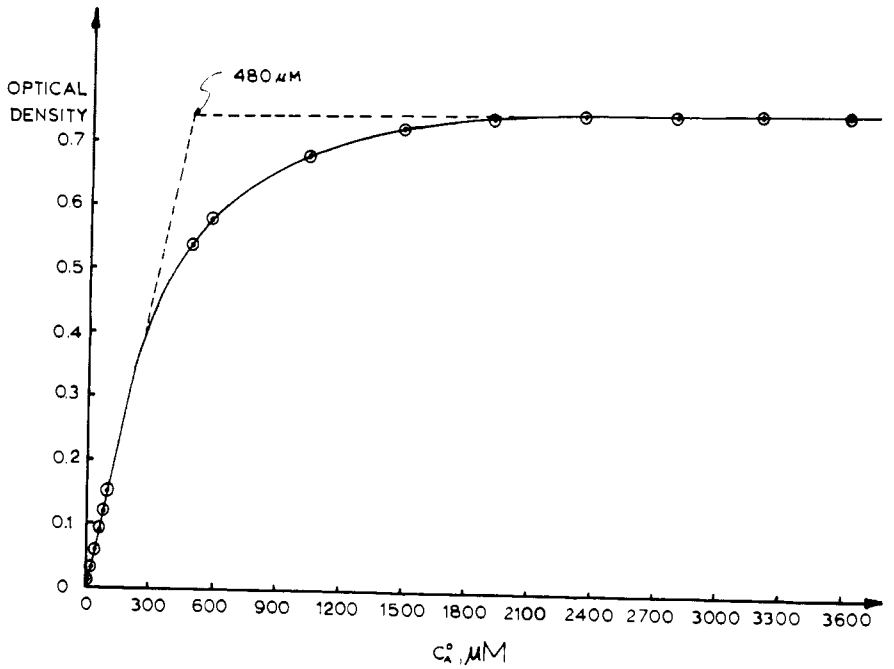

FIGURE 1: Titration of glutamic aspartic aminotransferase with β-hydroxyaspartic acid. From this experiment an enzyme concentration of 0.5 mM was derived. The inhibitory substrate was added with micropipets and the changes in transmission were determined with the Eppendorf photometer, employing a Schott double-band interference filter, peaking at 505 mμ. Borate buffer was used at *p*H 9.0 and ionic strength 0.1, 25°.

Results

General. In our mixture of glutamic aspartic aminotransferase and *erythro*-β-hydroxyaspartate, three different relaxation processes could easily be distinguished (Figures 2, 3, and 5). The various observables of the fastest relaxation process (indexed 1) were independent of the analytical concentrations of the reactants. The fastest process would then have to represent a monomolecular interconversion. The second fastest relaxation process (indexed 2) demonstrated the concentration dependence of an ordinary bimolecular reaction. The slowest relaxation process (indexed 3) appeared with a concentration dependence, which is characteristic of a slow monomolecular interconversion connected to a fast bimolecular recombination.

The simplest way of explaining these general results is to assume the presence of three individual reaction steps. Another simplificaton is introduced by assuming that only a single component is attributable to the absorption peak near 490 mμ. If this is done, the relaxation processes can be detected only via this component, temporarily denoted X. The fastest relaxation process then corresponds to a monomolecular interconversion between X and some other component. X or this mentioned component must then be connected to the bimolecular step which represents the combination of free enzyme, E, with free substrate, A. Either X or its fast-conversion product must then be identical with the first bimolecular association complex, EA. The slowest relaxation process then introduces another component which is connected in a monomolecular reaction to either X or its fast conversion product. These considerations thus lead to the following possible reaction schemes:

$$E + A \rightleftharpoons X \overset{\text{fast}}{\rightleftharpoons} Y \overset{\text{slow}}{\rightleftharpoons} Z \,(\rightleftharpoons E' + A') \quad (1)$$

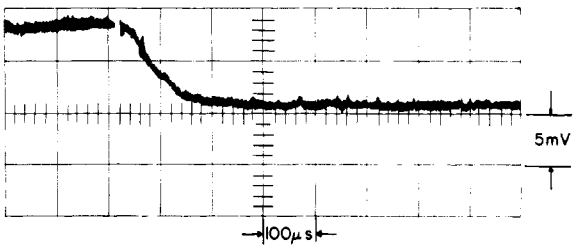

FIGURE 2: An oscilloscope trace of the shortest time constant without employing any electronic filtering system, using Tektronix oscilloscope type No. 545 with 53/54 D plug-in unit. c_E° = 0.234 mM, c_A° = 5 mM, borate buffer, *p*H 9.0, ionic strength 0.1, 20° initially.

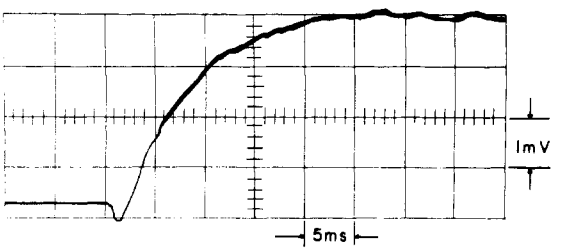

FIGURE 3: Oscilloscope trace of the second relation process. Rise-time constant = 500 μsec, delay time = 500 μsec, c_E° = 0.12 mM, c_A° = 0.5 mM, otherwise as in Figure 2.

$$E + A \rightleftharpoons EA \overset{\text{fast}}{\rightleftharpoons} X \overset{\text{slow}}{\rightleftharpoons} Y \; (\rightleftharpoons E' + A') \quad (2)$$

$$E + A \rightleftharpoons X \begin{cases} \xrightarrow{\text{fast}} Y \\ \xrightarrow{\text{slow}} Z \; (\rightleftharpoons E' + A') \end{cases} \quad (3)$$

$$E + A \rightleftharpoons EA \begin{cases} \xrightarrow{\text{fast}} X \\ \xrightarrow{\text{slow}} Y \; (\rightleftharpoons E' + A') \end{cases} \quad (4)$$

An experimental distinction cannot be derived from our results. But, if the first bimolecular component formed upon association of E and A is a diffusion complex (see the Discussion), it is quite unlikely that it has the strong absorption at the long wavelength, which requires considerable structural rearrangement for the formation of a new chromophoric configuration (see Figure 12 and its discussion following). If this is the case, reaction sequences (1) and (3) need not be considered any further. Reaction sequence (4) has a branching. Steady-state experiments of Jenkins (1961) have indicated that the turnover of the enzyme proceeds via the slow step, as indicated in all equations. Component X in reaction (4) would be in a "noncatalytic" side branch. Although such a reaction cannot be excluded, the full sequential type of scheme (2) appears much more attractive. Scheme (2) incorporates both monomolecular interconversions into the catalytic pathway. It also represents well the configurational picture of the various intermediates in the full aminotransferase system, as will be shown later (Figure 12).

Component Y in reactions (2) and (4) (or Z in reactions (1) and (3)) decomposes into the products E′ and A′. But the dissociation into E′ and A′ is so small that their concentrations can be neglected at the analytical concentrations of enzyme and substrate actually used. This reaction step was therefore placed in brackets.

Kinetics. Eigen (1954) originally introduced the concept of chemical relaxation (see also Eigen and De-Maeyer, 1963). Kinetics was more generally formulated in terms of analytical concentrations recently by Czerlinski (1964b). The specific equations employed here may be derived from the mentioned, more general ones by proper substitution. Therefore, only the final equations actually used are presented here.

After having selected scheme (2) one may introduce the six velocity constants:

$$E + A \underset{k_2}{\overset{k_1}{\rightleftharpoons}} EA \underset{k_4}{\overset{k_3}{\rightleftharpoons}} X \underset{k_6}{\overset{k_5}{\rightleftharpoons}} Y \quad (5)$$

The three equilibrium constants are then given by

$$K_{2,1} = \frac{k_2}{k_1} = \frac{\bar{c}_E \bar{c}_A}{\bar{c}_{EA}} \quad (6)$$

$$K_{4,3} = \frac{k_4}{k_3} = \frac{\bar{c}_{EA}}{\bar{c}_X} \quad (7)$$

$$K_{6,5} = \frac{k_6}{k_5} = \frac{\bar{c}_X}{\bar{c}_Y} \quad (8)$$

Equilibrium concentrations are denoted by a bar over the concentration symbol *c*. The relaxation time of the fastest process is then given by

$$\tau_1^{-1} = k_3 + k_4 \quad (9)$$

This result is very easily obtained (compare equation (2.15) of Czerlinski, 1964b, part I).

Figure 2 demonstrates the first relaxation process as seen on the oscilloscope with no electronic filtering network. The time constant of this fastest relaxation process was practically independent of the various concentrations used (10 μM $\leq c_E^\circ \leq$ 1000 μM; $c_A^\circ \geq c_E^\circ$). The evaluations lead to τ_1 = (50 ± 20) μsec. This is not the true relaxation time of the fast process as it is rather close to the heating time constant (around 10 μsec). Evaluation of the velocity constants gives, therefore, only lower limits: $k_3 > 2 \times 10^4$ sec$^{-1} \gg k_4$ or $k_4 > 2 \times 10^4$ sec$^{-1} \gg k_3$. Table I shows that consideration

TABLE I: Summary of Results from This Paper.

i	k_i (sec^{-1})	$K_{i,i-1}$	$\frac{\Delta K_{i,i-1}}{K_{i,i-1}}$	$\Delta H_{i,i-1}$ (kcal/mole)
2	72 ± 5	(0.45 ± 0.07) mM	0.02 ($\pm 50\%$)	1.6 (± 60)
4	$\gtrsim 2 \times 10^4$	5 ± 2	-0.021 ($\pm 5\%$)	1.7 (± 15)
6	0.4 ± 0.01	0.222 ± 0.009	0.047 ($\pm 12\%$)	3.8 (± 22)

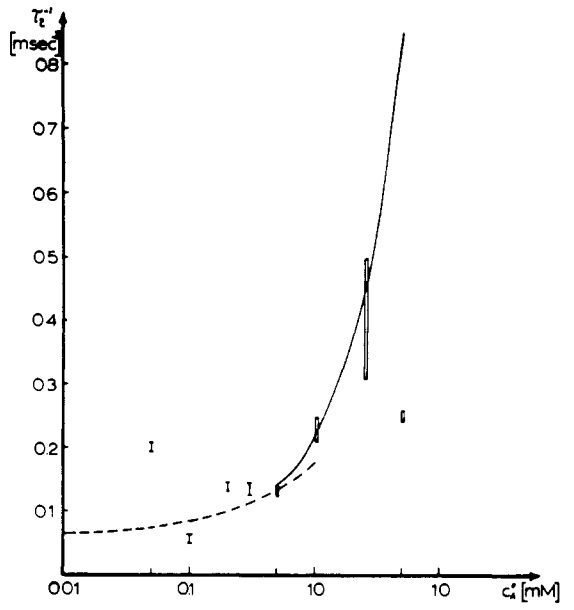

FIGURE 4: Summarizing plot $\tau_2^{-1} = f(c)_A^\circ$. Experimental points for $c_A^\circ \gg c_E^\circ = 0.12$ mM are indicated by blocks, while those for $c_A^\circ = c_E^\circ$ by vertical lines. The curves correspond to different theoretical equations; see text.

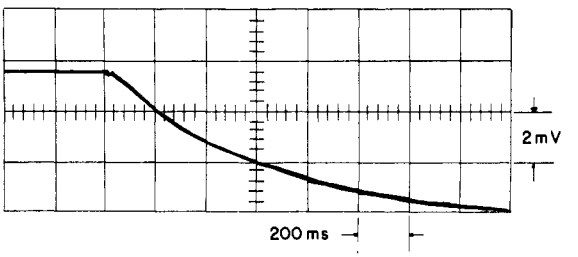

FIGURE 5: Oscilloscope trace of the slowest relaxation process. Rise-time constant = 20 msec; delay time = 25 msec; $c_E^\circ = 0.12$ mM; $c_A^\circ = 1$ mM; otherwise as in Figure 2.

of all data leads us to $k_4 \geq 2 \times 10^4$ sec^{-1}. Table I gives also a value for $K_{4,3}$, which certainly cannot be derived from (7) or (9). This equilibrium constant can be obtained only by successive approximation from all data, causing also the relatively large error. (That successive approximations could actually lead to $K_{4,3}$ becomes apparent from a comparison of the terms in equations (10) and (11) and of the terms in equations (12) and (13), *vide infra*.)

Experimental circumstances oblige us to remain within the *analytical* (denoted by superscript°) concentration range $10^{-5} < c_E^\circ < 10^{-3}$ M (if $c_E^\circ < 10^{-5}$ M, E′ and A′ can no longer be neglected; if $c_E^\circ > 10^{-3}$ M, the absorption of the solution is too large). In order to obtain sufficiently reliable results within this narrow concentration range, we therefore use two experimental conditions among the analytical concentrations, namely, $c_E^\circ \ll c_A^\circ$ and $c_E^\circ = c_A^\circ$. These experimental conditions lead also to the simplified equations for the observable parameters. One obtains for $c_E^\circ = c_A^\circ$:

$$\tau_2^{-1} = \frac{k_2}{1 + K_{3,4}} + k_1 \frac{K_{2,1}K_{4,3}}{1 + K_{4,3} + K_{5,6}} \times \left(\left[1 + \frac{4c_A^\circ(1 + K_{4,3} + K_{5,6})}{K_{2,1}K_{4,3}}\right]^{1/2} - 1\right) \quad (10)$$

and for $c_E^\circ \ll c_A^\circ$:

$$\tau_2^{-1} = \frac{k_2}{1 + K_{3,4}} + k_1 c_A^\circ \quad (11)$$

The last equation is identical with equation (5.2) of Czerlinski (1964b, part II) if c_1° there is replaced by c_A°.

An oscilloscope trace of the second relaxation process is shown in Figure 3; the first relaxation process has been grounded out as mentioned earlier. Figure 4 gives a plot of $\tau_2^{-1} = f(c_A^\circ)$. Theoretical curves are drawn, taking the values from Table I, and from equations (10) and (11) for the conditions. The scattering for concentration equality is much larger than for concentration difference. The point for $c_A^\circ = 50$ μM is rather doubtful (concentrations of A′ and E′ are no longer negligible compared to that of Y). Similar doubt is associated with the point at $c_A^\circ = 5$ mM (A reacts with E′? See discussion of a paper by Jenkins, 1964).

The slowest relaxation time may be derived from (3.9) of Czerlinski (1964b), part II, if $K_{2,1}$ there is replaced by $K_{2,1}(1 + K_{3,4})^{-1}$ and $\bar{c}_1 \to \bar{c}_A$, $\bar{c}_2 \to \bar{c}_E$. If $c_A^\circ \gg c_E^\circ$, one obtains

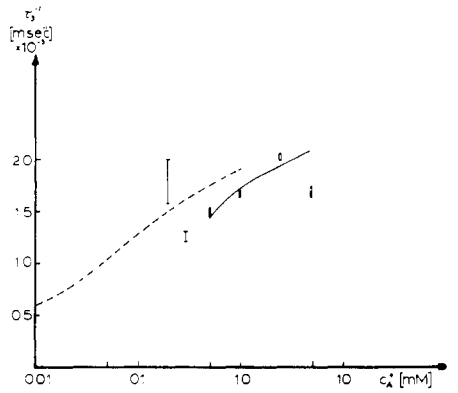

FIGURE 6: Summarizing plot $\tau_3^{-1} = f(c_A^\circ)$. Experimental points for $c_A^\circ \gg c_E^\circ = 0.12$ mM are indicated by blocks, while those for $c_A^\circ = c_E^\circ$ by vertical lines. The curves correspond to different theoretical equations; see text.

$$\tau_3^{-1} = k_6 + k_5 \frac{c_A^\circ}{K_{2,1}(1 + K_{3,4})^{-1} + c_A^\circ} \qquad (12)$$

If $c_A^\circ = c_E^\circ$, then also $\bar{c}_A = \bar{c}_E$. Here $\bar{c}_A$ has to be substituted by an expression containing only analytical concentrations. One finally obtains

$$\tau_3^{-1} = k_6 + k_5 \left[1 + \left(\frac{K_{5,6}}{1 + K_{4,3}}\right) \times \left(\left[1 + \frac{4c_A^\circ(1 + k_{4,3} + k_{5,6})}{K_{2,1}K_{4,3}}\right]^{1/2} - 1\right)^{-1}\right]^{-1} \qquad (13)$$

Figure 5 shows an oscilloscope trace of the third relaxation process (using again the above-mentioned grounding circuit). A plot of τ_3^{-1} as a function of c_A° is given in Figure 6. Equations (12) and (13) have been used for the theoretical curve together with the parameters from Table I. Only two points could be determined for $c_A^\circ = c_E^\circ$. These points scatter somewhat around the theoretical curve.

The experiments were performed in sodium borate buffer, *p*H 9. Some experiments were also conducted at *p*H 8 with borate or potassium phosphate as buffer. As there was negligible difference compared to the experiments at *p*H 9, the effects of the hydrogen ion concentration were not considered further.

Statics. Statics of chemical relaxation describes the signal obtained with the enzyme-substrate mixture in the apparatus, in which the temperature jumps are also performed. In transmission, one observes a reference signal S_o, if no indicating component is present. With the full mixture, the detected signal S_T obeys the relationship $S_o > S_T$. As long as only one component X is assumed to absorb and the product of optical path length and extinction coefficient is sufficiently small so that the optical signal change is linear in this quantity, it is:

$$S_o - S_T = \eta_X \bar{c}_X \qquad (14)$$

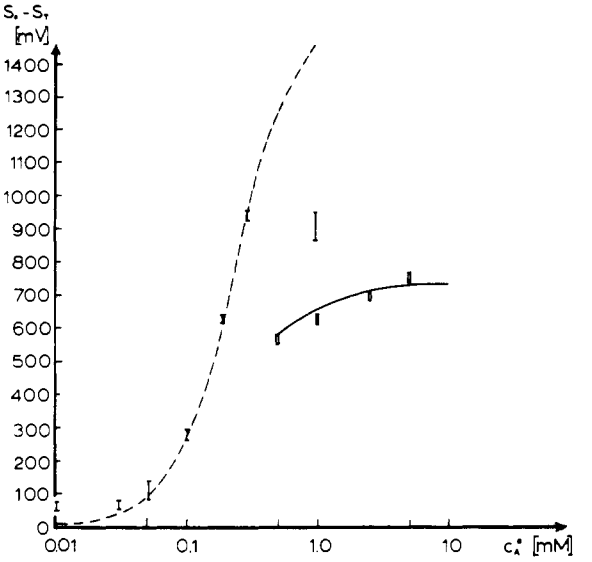

FIGURE 7: Summarizing plot of $S_o - S_T = f(c_A^\circ)$. Experimental points for $c_A^\circ \gg c_E^\circ = 0.12$ mM are indicated by blocks, while those for $c_A^\circ = c_E^\circ$ by vertical lines. The curves correspond to different theoretical equations; see text.

The coefficient η_X is the characteristic signal of component X (given in volt per molar concentration).

The analytical concentrations c_E° and c_A° may be written in terms of the equilibrium concentrations. These expressions and equations (6), (7), and (8) allow solving for the individual equilibrium concentrations in terms of analytical concentrations only. One obtains for the experimental condition $c_A^\circ \gg c_E^\circ$:

$$\bar{c}_X = \frac{c_A^\circ c_E^\circ}{c_A^\circ(1 + K_{4,3} + K_{5,6}) + K_{2,1}K_{4,3}} \qquad (15)$$

Similarly, one may solve for c_A° and obtain for the condition $c_A^\circ = c_E^\circ$:

$$\bar{c}_A = \frac{\frac{1}{2}K_{2,1}K_{4,3}}{1 + K_{4,3} + K_{5,6}} \times \left(\left[1 + \frac{4c_A^\circ(1 + K_{4,3} + K_{5,6})}{K_{2,1}K_{4,3}}\right]^{1/2} - 1\right) \qquad (16)$$

Equation (16) may be used to arrive at another expression for $\bar{c}_X$ (with $c_A^\circ = c_E^\circ$):

$$\bar{c}_X = \frac{c_A^\circ}{1 + K_{4,3} + K_{5,6}} - \frac{\frac{1}{2}K_{2,1}K_{4,3}}{(1 + K_{4,3} + K_{5,6})^2} \times \left(\left[1 + \frac{4c_A^\circ(1 + K_{4,3} + K_{5,6})}{K_{2,1}K_{4,3}}\right]^{1/2} - 1\right) \qquad (17)$$

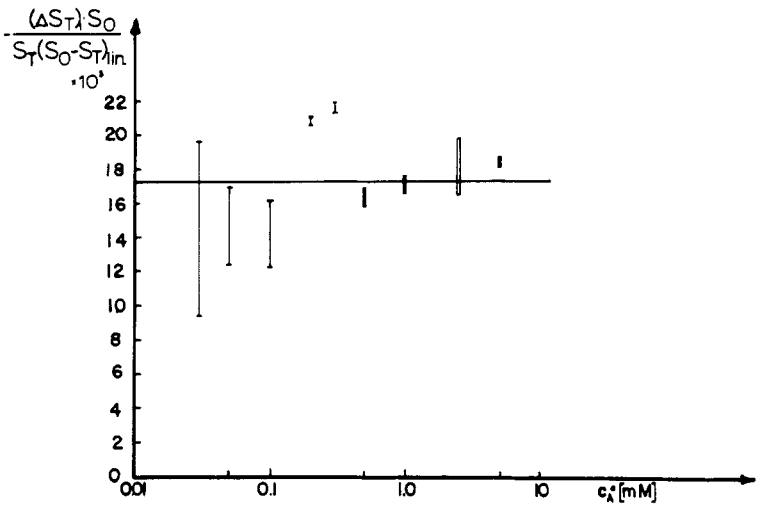

FIGURE 8: Presentation of $\frac{(\Delta S_T)_1}{S_T} \cdot \frac{S_o}{(S_o - S_T)_{lin}}$ as a function of c_A°. Experimental points for $c_A^\circ \gg c_E^\circ = 0.12$ mM are indicated by blocks while those for $c_A^\circ = c_E^\circ$ by vertical lines. The curves correspond to different theoretical equations; see text.

Figure 7 represents a graph of $S_o - S_T$ as a function of c_A°. The dashed curve represents the condition $c_A^\circ = c_E^\circ$, employing equations (14) and (17). The full curve is valid for the condition $c_A^\circ \gg c_E^\circ = 121.5$ μM, employing equations (14) and (15). All theoretical curves employ the data obtained from kinetics (Table I) and use $\eta_X = 95.6$ mv μM^{-1}.

Thermodynamics. Since only one component is assumed to absorb, the observed total signal change ΔS_T is related to the concentration change of the indicating component by

$$\Delta S_T = -S_T 2.3 \epsilon_X l \, \Delta \bar{c}_X \tag{18}$$

This equation is generally valid owing to a basic condition for chemical relaxation ($\Delta \bar{c}_X \ll \bar{c}_X$). The negative sign results from the fact that an increase in the concentration of X is associated with a decrease in the transmitted signal.

There are three different relaxation processes and thus there must be three different $\Delta \bar{c}_X$. The fastest concentration change, $(\Delta \bar{c}_X)_1$, may be derived from equation (8.2) of Czerlinski (1964b), which here becomes

$$\frac{\Delta K_{4,3}}{K_{4,3}} = -\frac{(\Delta \bar{c}_X)_1}{\bar{c}_X}(1 + K_{3,4}) \tag{19}$$

The van't Hoff equation then introduces the enthalpy $\Delta H_{4,3}$. For practical purposes one has to multiply (18) with $S_o(S_T[S_o - S_T])^{-1}$, which results with equation (14) in:

$$\frac{(\Delta S_T)_1}{S_T} \cdot \frac{S_o}{S_o - S_T} = -\frac{(\Delta \bar{c}_X)_1}{\bar{c}_X} \tag{20}$$

If one solves equation (19) for $(\Delta \bar{c}_X)_1$ and inserts this value into equation (20), it is apparent that the latter is independent of c_A°, as is reasonably well demonstrated in Figure 8 for both conditions $c_A^\circ = c_E^\circ$ and $c_A^\circ \gg c_E^\circ$. The best fit to all data results in $\Delta K_{4,3}/K_{4,3} = -0.021$, which gives $\Delta H_{4,3} = -1.7$ kcal/mole, with $\Delta T = 2.1$ C and $T = 293$ K.

To find an expression for $(\Delta \bar{c}_X)_2$, one must proceed as shown formerly (Czerlinski, 1964b, chap. VII). Equation (7.7) of the cited reference is applicable here; using the indices of this paper, former equation (7.7) reads:

$$\frac{(\Delta \bar{c}_X)_2}{\bar{c}_X} = -\frac{K_{2,1}\frac{\Delta K_{2,1}}{K_{2,1}} + \frac{\Delta K_{4,3}}{K_{4,3}}[K_{2,1} + c_A^\circ + c_E^\circ - 2\bar{c}_X(1 + K_{4,3})]}{K_{2,1} + (1 + K_{3,4})[c_A^\circ - c_E^\circ - 2\bar{c}_X(1 + K_{4,3})]} \tag{21}$$

This equation is particularly useful for the experimental condition $c_A^\circ \gg c_E^\circ$, where $c_E^\circ > \bar{c}_X(1 + K_{4,3})$ also. It then becomes:

$$\frac{(\Delta \bar{c}_X)_2}{\bar{c}_X} = -\frac{K_{2,1}\left(\frac{\Delta K_{2,1}}{K_{2,1}} + \frac{\Delta K_{4,3}}{K_{4,3}}\right) + \frac{\Delta K_{4,3}}{K_{4,3}} c_A^\circ}{K_{2,1} + (1 + K_{3,4})c_A^\circ} \tag{22}$$

$$c_A^\circ \xrightarrow{\lim} 0 \quad \frac{(\Delta \bar{c}_X)_2}{\bar{c}_X} = -\frac{\Delta K_{2,1}}{K_{2,1}} - \frac{\Delta K_{4,3}}{K_{4,3}} \tag{23}$$

$$c_A^\circ \xrightarrow{\lim} \infty \quad \frac{(\Delta \bar{c}_X)_2}{\bar{c}_X} = -\frac{\Delta K_{4,3}}{K_{4,3}}(1 + K_{3,4})^{-1} \tag{24}$$

One may finally introduce the enthalpies $\Delta H_{2,1}$ and

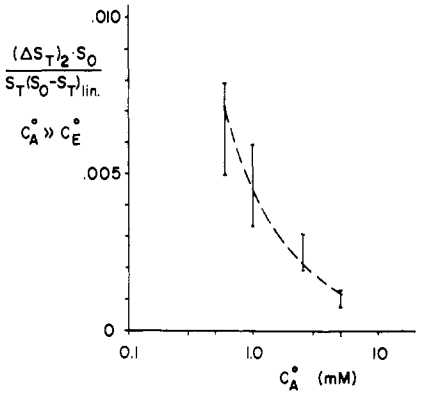

FIGURE 9: Presentation of $\frac{(\Delta S_T)_2}{S_T} \cdot \frac{S_o}{(S_o - S_T)_{lin}}$ as a function of c_A°, for $c_A^\circ \gg c_E^\circ = 0.12$ mM. The curves corresponds to a theoretical equation; see text.

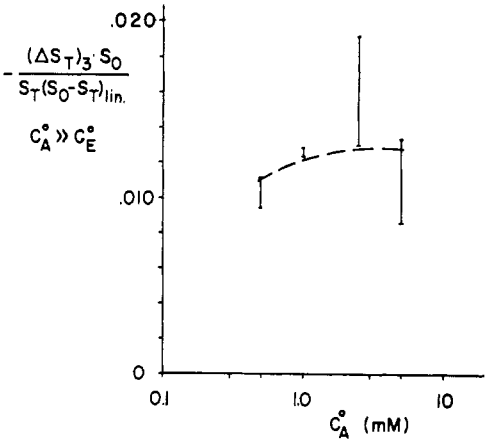

FIGURE 10: Presentation of $\frac{(\Delta S_T)_3}{S_T} \cdot \frac{S_o}{(S_o - S_T)_{lin}}$ as a function of c_A°, for $c_A^\circ \gg c_E^\circ = 0.12$ mM. The curve corresponds to a theoretical equation; see text.

$\Delta H_{4,3}$. For practical purposes, one then writes the equilibrium change of the second step similar to (20):

$$\frac{(\Delta S_T)_2}{S_T} \frac{S_o}{S_o - S_T} = -\frac{(\Delta \bar{c}_X)_2 - (\Delta \bar{c}_X)_1}{\bar{c}_X} \tag{25}$$

with $S_o - S_T$ obtained from Figure 7 (full curve). It is thus possible to plot the left-hand side of equation (25) as a function of c_A° (at fixed c_E°) and to draw into it a theoretical curve, given by (25). This has been done in Figure 9, with $\Delta K_{2,1}/K_{2,1} = 0.02$, corresponding to $\Delta H_{2,1} = 1.6$ kcal/mole.

If condition $c_A^\circ = c_E^\circ$ prevails, one must combine equation (21) with equation (17). This combination results in an equation which is rather complex for practical purposes and will therefore not be given.

The thermodynamics for the third relaxation process will now be derived. One must employ the equations:

$$\frac{\Delta K_{2,1}}{K_{2,1}} = \frac{\Delta \bar{c}_E}{\bar{c}_E} + \frac{\Delta \bar{c}_A}{\bar{c}_A} - \frac{\Delta \bar{c}_{EA}}{\bar{c}_{EA}} \tag{26}$$

$$\frac{\Delta K_{4,3}}{K_{4,3}} = \frac{\Delta \bar{c}_{EA}}{\bar{c}_{EA}} - \frac{\Delta \bar{c}_X}{\bar{c}_X} \tag{27}$$

$$\frac{\Delta K_{6,5}}{K_{6,5}} = \frac{\Delta \bar{c}_X}{\bar{c}_X} - \frac{\Delta \bar{c}_Y}{\bar{c}_Y} \tag{28}$$

$$\Delta \bar{c}_E = \Delta \bar{c}_A = -(\Delta \bar{c}_{EA} + \Delta \bar{c}_X + \Delta \bar{c}_Y) \tag{29}$$

These equations lead to

$$\frac{(\Delta \bar{c}_X)_3}{\bar{c}_X} = \frac{(\bar{c}_A + \bar{c}_E)K_{1,2}\left(K_{3,4}K_{5,6}\frac{\Delta K_{6,5}}{K_{6,5}} - \frac{\Delta K_{4,3}}{K_{4,3}}\right) - \frac{\Delta K_{4,3}}{K_{4,3}} - \frac{\Delta K_{2,1}}{K_{2,1}}}{1 + K_{1,2}(\bar{c}_A + \bar{c}_E)[1 + K_{3,4}(1 + K_{5,6})]} \tag{30}$$

For $c_A^\circ \gg c_E^\circ$ one obtains $c_A^\circ \approx \bar{c}_A \gg \bar{c}_E$ and:

$$\frac{(\Delta \bar{c}_X)_3}{\bar{c}_X} = \frac{\left(K_{3,4}K_{5,6}\frac{\Delta K_{6,5}}{K_{6,5}} - \frac{\Delta K_{4,3}}{K_{4,3}}\right)K_{1,2}c_A^\circ - \frac{\Delta K_{4,3}}{K_{4,3}} - \frac{\Delta K_{2,1}}{K_{2,1}}}{1 + [1 + K_{3,4}(1 + K_{5,6})]K_{1,2}c_A^\circ} \tag{31}$$

$$\lim_{c_A^\circ \to 0} \frac{(\Delta \bar{c}_X)_3}{\bar{c}_X} = -\frac{\Delta K_{2,1}}{K_{2,1}} - \frac{\Delta K_{4,3}}{K_{4,3}} \tag{32}$$

$$\lim_{c_A^\circ \to \infty} \frac{(\Delta \bar{c}_X)_3}{\bar{c}_X} = \frac{K_{3,4}K_{5,6}\frac{\Delta K_{6,5}}{K_{6,5}} - \frac{\Delta K_{4,3}}{K_{4,3}}}{1 + K_{3,4}(1 + K_{5,6})} \tag{33}$$

Equation (32) is identical with (23). The relation to the signal change becomes:

$$\frac{(\Delta S_T)_3}{S_T} \cdot \frac{S_o}{S_o - S_T} = \frac{(\Delta \bar{c}_X)_3 - (\Delta \bar{c}_X)_2}{\bar{c}_X} \tag{34}$$

where $S_o - S_T$ is obtainable from Figure 7 (full curve).

Figure 10 gives a plot of the left side of equation (34) as a function of c_A°. The theoretical curve is obtained from (34) with (31), (22), (15), the data given previously, and $\Delta K_{6,5}/K_{6,5} = 0.047$, corresponding to $\Delta H_{6,5} = 3.8$ kcal/mole.

The condition $c_A^\circ = c_E^\circ$ results in $\bar{c}_A = \bar{c}_E$, but gives little simplification of (30). For $\bar{c}_A$ one must then introduce the expression of equation (16). The final expression becomes so complex, however, that its use seems impractical. In order to give a better overall view, the results are summarized in Table I with the enthalpies of the various steps in the last column.

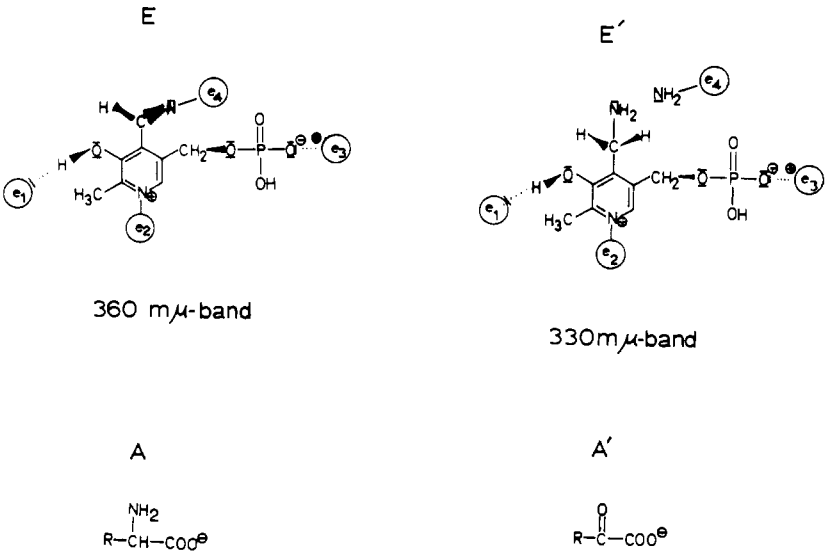

FIGURE 11: Two-dimensional representations of the stereochemistry of the two forms of aminotransferases. Bonds (essential) in or parallel to the plane of writing have constant thickness; bonds at an angle to the plane have changing thickness, and are widest where they point upward out of the plane. One side of these lines is generally within the plane of writing. The e_i are particular binding sites of the enzymes.

Discussion

Three different relaxation processes are present, and this fact demonstrates the presence of three different reactions. They are all coupled kinetically to the compound absorbing at 492 mμ. From four possibilities (equations 1 to 4), mechanism (2) was selected, and the theoretical assumptions connected with this mechanism could be shown to agree reasonably well with the experiments. The presence of more than three intermediates cannot be excluded, and even seems quite probable on the grounds of the configurations one could develop for the whole mechanism.

A two-dimensional representation of possible structures for the two enzyme forms is suggested in Figure 11. The maximum possible number of enzymatic ligands, e_i, is indicated. No evidence is available for e_1 as yet. Actually, at *p*H 9, the phenolic proton is expected to be dissociated (and e_1 – H at low *p*H may just be structural H_2O as well). But Hammes and Fasella (1963) could derive from the slow dissociation of the proton ($pK_H \backsimeq 6.25$) that it is structurally bound (hydrogen bonded). The nature of e_2 is unknown, but some bond seems to be necessary to permit the establishment of a quinoid structure (see Figure 12). Whether e_3 is actually on the enzyme (as an $-NH_3^+$?) or whether the phosphate group is protruding from the surface of the enzyme cannot be decided yet. Some e_3 of the enzyme would largely fix the orientation of the pyridoxamine on the enzyme, but such an orientation would not be necessary for enzyme specificity according to present knowledge; stereospecificity may be established by the proper attachment of the substrate to the enzyme. NH_2 at e_4 is the ε-amino group of a lysine residue (Turano *et al.*, 1961; Hughes *et al.*, 1962). The Schiff-base nitrogen may actually be protonated, according to Cordes and Jencks (1962). The protonation state of some of the groups may be different from the indicated one, but there seems to be no change in the protonation state over the whole reaction, since no *p*H dependence of the relaxation processes in the range considered was evident.

This mentioned *p*H independence of the whole reaction at higher *p*H was also found by Jenkins (1964). To explain it, the enzymatic group e_5 (imidazole?) was introduced in the suggested overall mechanism of Figure 12. This group provides an *intra*molecular proton transfer, which is practically inaccessible to the outside. In Figure 12, three substituents of the pyridine ring are omitted for simplicity. The possibility that $e_5 = e_1$ plus OH of the pyridine ring is not excluded. It is demonstrated in the figure that the 492 mμ absorption band of component X is attributed to an electromeric system. Although the wavelength shift of the absorption band is large, it is not assumed to be attributable to an electron-transfer complex.

All the reactions involving this enzyme and *natural* substrates seem to be rather fast, according to Hammes and Fasella (1962), who performed temperature-jump experiments with detection between 300 and 400 mμ. Table II summarizes the results of Hammes and Fasella (1962). In comparing the two tables, one should keep in mind that Hammes and Fasella used phosphate buffer (*p*H 8, high ionic strength), while the present authors used borate buffer (*p*H 9, medium ionic strength).

The K_{diss} in Table II represents the constant of dissociation of the indicated binary complex into its components. The very first dissociation constant is surprisingly close to $K_{2,1}$ of Table I. But the rate con-

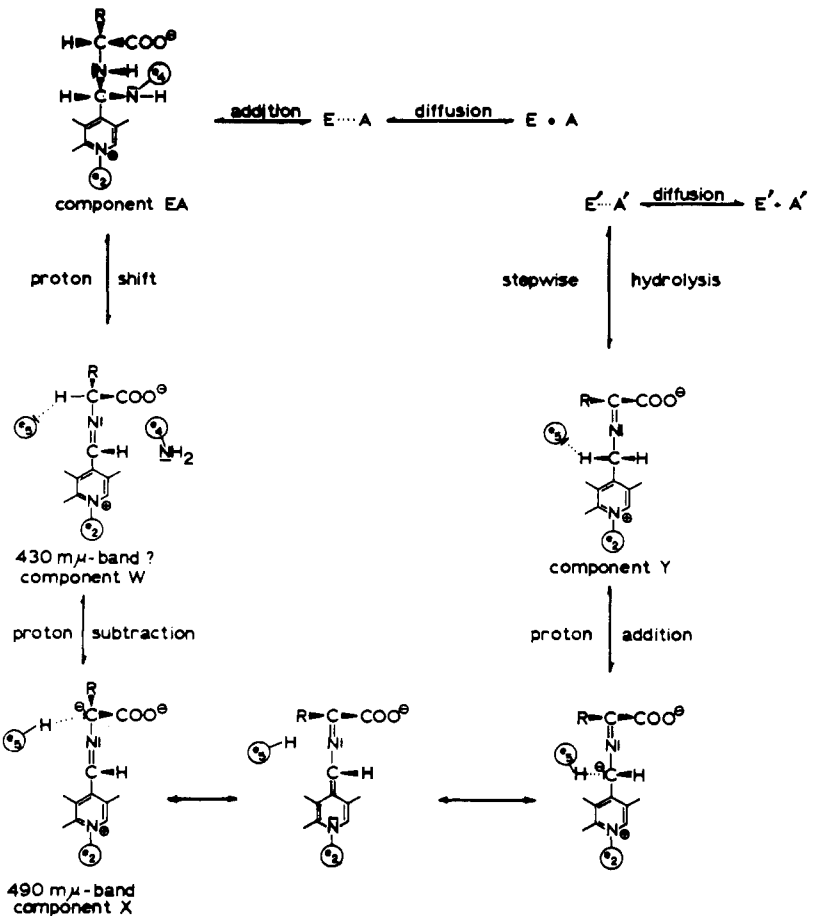

FIGURE 12: Two-dimensional representation of the stereochemistry of intermediates in the reaction scheme. For explanation see Figure 11 and the text.

TABLE II: Summary of Results of Hammes and Fasella (1962).

Binary Complex with Enzyme Form	K_{diss} (μM)	k_{diss} (sec^{-1})	$k_{interconv}$ (sec^{-1})
Schiff base–aspartate	550	$>5 \times 10^3$	80
Pyridoxamine-oxalacetate	2	140	26
Pyridoxamine-ketoglutarate	3.3	70	30
Schiff base–glutamate	85	2.8×10^3	61

stant for dissociation of this binary complex in Table II is considerably larger than k_2. One may infer that the *erythro*-hydroxy group slows both rate constants in this association process by about the same amount. The k_3 and k_4 are probably of the same magnitude in the natural systems. In the natural system they can probably not be detected, however, because their time response is too close to that of the bimolecular association step.

All four monomolecular constants associated with the two monomolecular interconversions of equation (2) and derivable from Table I are quite different from the interconversion rate constants of Table II. Rate constant k in the last column of Table II refers to that monomolecular rate constant, converting the listed binary complex to the "other" binary complex of the half-reaction; Hammes and Fasella (1962) could only derive two binary complexes from their experiments on the half-reactions of this aminotransferase.

It is not known which one of the steps between E . . . A and X in Figure 12 is time limiting for τ_1. It is probably the interconversion between (the newly introduced) component W and X. Only a "differential double-beam temperature-jump apparatus" might be capable of resolving this problem (in such an apparatus, identical temperature-jump experiments are performed simultaneously, but observed at different wavelengths differentially). Several years could pass before such an apparatus becomes available so that this question must await later investigations.

The second relaxation process showed strong con-

centration dependence and was attributed to the diffusion step. The bimolecular velocity constant was experimentally found to be $k_1 = 1.6 \times 10^5$ M^{-1} sec^{-1}, which is considerably below the value one might expect for diffusion-limited reactions. It is very difficult to believe that k_1 *is* the true bimolecular diffusion-limited velocity constant and that it is so small because of stringent steric requirements (only a *very* small number of molecular encounters are sterically acceptable).

Even if there are many encounters which are unsuccessful for reaction, the lifetime of some of the encounter complexes may not be negligible. This leads to the second possibility, in which one has to *add* to reaction (2) the competitive reaction (competition for A: $\overline{\text{EA}}$ contains A not bound (exactly) at active site).

$$\text{E} + \text{A} \underset{k_8}{\overset{k_7}{\rightleftarrows}} \overline{\text{EA}} \tag{35}$$

The velocity constant k_7 (and k_8?) may then be largely diffusion determined. If $K_{8,7}$ becomes sufficiently small, however, and if there are many competitive binding sites per enzyme molecule, equation (35) could lead to a severe reduction in the amount of free substrate, and the "true" k_1 is larger than the value given. The problem can be solved by using different ratios c_E°/c_A° for experimentation. Such experiments were actually performed by employing the conditions $c_E^\circ = c_A^\circ$ *and* $c_E^\circ \ll c_A^\circ$. The results demonstrated little difference. This possibility can therefore be neglected until further and more precise experimental data are available.

A third possibility is suggested by the presence of several intermediates between ER and X, as given in Figure 12. One should then expect that τ_2^{-1} would reach a plateau at high c_A°. This could, in fact, be the case, as visible from Figure 4. The uncertainty of this point, however, does not justify an even more complex analysis. Also, if the concentrations of these intermediates are sufficiently small, additional relaxation times could not be uncovered via component X. One would have to attempt detection via components present in relatively *small* concentrations.

Finally, as a fourth possibility, one may consider that the enzyme is present in two forms which are in a very fast equilibrium:

$$\text{E} \underset{k''}{\overset{k'}{\rightleftarrows}} \text{F} \underset{k_2}{\overset{k_1'}{\rightleftarrows}} \underset{\text{A}}{\text{EA}} \tag{36}$$

Then A reacts only with form F, which is present at very low concentration. If $\bar{c}_E/\bar{c}_F = 10^3$, the amount of F would not show up with ordinary analytical tools. If $k'' = 10^7$ sec^{-1}, then the monomolecular step becomes much faster than the bimolecular one: $\tau_2' \gg \tau_1' = (k' + k'')^{-1}$. A system similar to equation (36) has been treated earlier (part II of Czerlinski, 1964b). One obtains

$$(\tau_2')^{-1} = k_2 + k_1' \frac{k'}{k''}\left(\bar{c}_E + \bar{c}_A \frac{1}{1 + k'/k''}\right) \tag{37}$$

with the proper modifications. Since $k'/k'' \ll 1$, the ordinary expression for a bimolecular recombination employing equilibrium concentrations is obtained. The former velocity constant k_1 must then be expressed by

$$k_1 = k_1' \frac{k'}{k''} \tag{38}$$

where k_1' is the diffusion-limited constant, now in the "appropriate" range of 2×10^8 M^{-1} sec^{-1}. Thus the presence of two forms of the enzyme could explain the low value of k_1.

The third relaxation process showed weak concentration dependence, and is several orders of magnitude slower than in systems with natural substrates. The *erythro*-β-hydroxy substituent of aspartic acid is evidently most effective here in slowing the reaction. This substituent then seems to affect strongly the transfer of the proton from $e_5 - \text{H}$ to the electromeric system. This OH group could therefore be rather close to enzyme site e_5. It is also possible that the withdrawal of a proton for the formation of $e_5 - \text{H}$ is influenced by this OH group, but sufficient data to substantiate this idea are not as yet available.

It is evident that component Y is only weakly hydrolyzed, leading to relatively small equilibrium concentrations of E′ and A′. Unfortunately, A′ is not very stable but slowly degenerates further, which affects the reliability of the experiments under the condition $c_E^\circ = c_A^\circ$. Instrumental attachments to diminish the influence of such effects are in development. Jenkins (1961) found a value of 1.7 sec^{-1} (at 30°) as slowest monomolecular constant for the conversion of A to A′, a value which is rather close to our k_5 of 1.8 sec^{-1}. Jenkins (1964) also determined an overall dissociation constant, for which he found 0.38 mM. From our data we obtained an overall dissociation constant of 0.22 mM. The deviation of 40% is explained on the grounds that we assume only the L isomer to be enzymatically active. Differences in the purity of the enzyme may also have caused some deviations.

Jenkins (1964) also mentions the presence of abortive complexes: E reacting with A′, and E′ reacting with A. The relative dissociation constants of these complexes are such that they could explain well the deviation of our experimental data from the theoretical curves at very low and very high analytical concentrations. In the same paper Jenkins derived that 58% of the binary complexes are on the Schiff-base side of the slowest step. One derives from equations (7), (8), and Table I that our results lead to 57%, in unusually good agreement with the results of Jenkins (1964).

Although these investigations with chemical relaxation methods have clearly revealed at least three different intermediates, it was shown in the discussion that the system might be more complicated than assumed thus far. Further improvement and refinement in the instrumentation should permit us to uncover more details. Since the natural system also shows absorption near

492 mμ (Jenkins, 1964), one may investigate this in more detail. One has to cope with an absorption, however, which is in the natural system much smaller than in the one employing the hydroxylated aspartic acid.

Acknowledgment

The authors gratefully acknowledge the generous cooperation of W. T. Jenkins in supplying the materials and some data before publication.

References

Cordes, E. H., and Jencks, W. P. (1962), *Biochemistry 1*, 773.

Czerlinski, G. (1962), *Rev. Sci. Instr. 33*, 1184.

Czerlinski, G. (1964a), *Ber. Bunsenges. Physik. Chem. 68*, 754.

Czerlinski, G. (1964b), *J. Theoretical Biol. 7* (Parts I and II), 435.

Czerlinski, G., and Eigen, M. (1959), *Z. Elektrochem. 63*, 652.

Czerlinski, G., Malkewitz, J., and Jenkins, W. T. (1964), Sixth International Congress of Biochemistry, New York, Abstract IV-35.

Czerlinski, G., and Nadler, W. (1965), *J. Sci. Instr.* (in press).

Czerlinski, G., and Schreck, G. (1964), *J. Biol. Chem. 239*, 913.

Eigen, M. (1954), *Discussions Faraday Soc. 17*, 194.

Eigen, M., and DeMaeyer, L. (1963), *Tech. Org. Chem. 11*, 895.

Hammes, G. G., and Fasella, P. (1962), *J. Am. Chem. Soc. 84*, 4644.

Hammes, G. G., and Fasella, P. (1963), *J. Am. Chem. Soc. 85*, 3929.

Hughes, R. C., Jenkins, W. T., and Fascher, E. H. (1962), *Proc. Natl. Acad. Sci. U.S. 48*, 1615.

Jenkins, W. T. (1961), *J. Biol. Chem. 236*, 1121.

Jenkins, W. T. (1963), *in* Proceedings of the Symposium on Chemical and Biological Aspects of Pyridoxal Catalysis, Rome, 1962, Pergamon, London, p. 139.

Jenkins, W. T. (1964), *J. Biol. Chem. 239*.

Turano, C., Fasella, P., Vechini, P., and Giartosio, A. (1961), *Atti. Accad. Nazl. Lincei, Rend. Classe Sci. Fis. Mat. Nat. 30*, 532.

Velick, S. F., and Vavra, J. (1962), *J. Biol. Chem. 237*, 2109.